

## LOCAL PIEZOELECTRICITY IN SrTiO<sub>3</sub>-BiTiO<sub>3</sub> CERAMICS

R. Grigalaitis <sup>a</sup>, Š. Bagdzevičius <sup>a</sup>, J. Banys <sup>a</sup>, E.E. Tornau <sup>b</sup>, K. Bormanis <sup>c</sup>, A. Sternberg <sup>c</sup>,

I. Bdikin <sup>d,e</sup>, and A. Kholkin <sup>d</sup>

<sup>a</sup> Faculty of Physics, Vilnius University, Saulėtekio 9, LT-10222 Vilnius, Lithuania

<sup>b</sup> Center for Physical Sciences and Technology, A. Goštauto 11, LT-01108 Vilnius, Lithuania

<sup>c</sup> Institute of Solid State Physics, University of Latvia, Kengaraga 8, LV-1063 Riga, Latvia

<sup>d</sup> Department of Ceramics and Glass Engineering/CICECO, University of Aveiro, 3810-193 Aveiro, Portugal

<sup>e</sup> Department of Mechanical Engineering/TEMA, University of Aveiro, 3810-193 Aveiro, Portugal

Received 5 June 2014; revised 14 July 2014; accepted 23 September 2014

Local piezoelectric properties of Bi-doped SrTiO<sub>3</sub> ceramics have been investigated by piezoresponse force microscopy. The appearance of both out-of-plane and in-plane polarization components confirmed the piezoelectric nature of the obtained signal. The absence of labyrinth-like structures in observed piezoelectric contrast is not consistent with the expected existence of a relaxor ferroelectric state in this material. The close similarity of local piezoelectric properties in Bi-doped SrTiO<sub>3</sub> with pure SrTiO<sub>3</sub> suggests that the origin of obtained piezoresponse can be attributed to the flexoelectric phenomenon. Bi-doping leads to occurrence of oxygen vacancies and negative charge on the surface of the sample.

**Keywords:** piezoelectric, piezoresponse force microscopy, flexoelectric, ferroelectric relaxor

**PACS:** 77.84.-s, 07.79.Lh, 77.65.Ly, 77.80.Jk

### 1. Introduction

Strontium titanate (SrTiO<sub>3</sub>) is one of the most popular incipient ferroelectric materials retaining its centrosymmetric structure even below the cubic-to-tetragonal phase transition at ~105 K [1]. This transition is caused by the antiphase rotations of the oxygen octahedra around one of the [001] crystallographic directions. The rotations double the unit cell of this material [2]. Ferroelectric state in SrTiO<sub>3</sub> can be induced by the application of a biaxial strain [3] or by the substitution of the A-site ions by isovalent Ba<sup>2+</sup>, Pb<sup>2+</sup>, Ca<sup>2+</sup>, Mn<sup>2+</sup> [4–6] or heterovalent La<sup>3+</sup>, Gd<sup>3+</sup>, Y<sup>3+</sup>, Bi<sup>3+</sup> ions [7–9]. These dopants not only alter the transition temperature but also can induce dipolar glass or ferroelectric relaxor state. This is not surprising because, in the case of substitution of Sr by heterovalent ions, only two of three atoms can be placed in the A-site positions and one void is left to satisfy the charge neutrality condition. The isovalent doping considerably affects the cubic-to-tetragonal transition temperature  $T_c$ . The transition temperature  $T_c$  decreases with increase of the Goldschmidt tolerance factor  $t$  for the most of heterovalent dopants (Y,

Ga, La) and Bi-doped solid solutions as well, though the lattice parameter of the latter system increases with bismuth content as opposed to Y, Ga, and La containing solid solutions. Such discrepancy was explained [10, 11] through the increase in the radius of Sr vacancy, being larger than the radii of both Bi and Sr ions. The structural transformations considerably affect the dielectric properties of Bi-doped SrTiO<sub>3</sub>. Skanavi et al. discovered [8] that (Sr<sub>1-1.5x</sub>Bi<sub>x</sub>)TiO<sub>3</sub> ceramics with moderate Bi content exhibit frequency dispersion similar to relaxor ferroelectrics (RF) and tried to explain this behaviour by using the hopping ion model. Later broadband dielectric studies on this material (up to  $x \leq 0.13$ ) [9] showed that Bi doping induces formation of local antiferrodistortive and polar regions. This causes a complex relaxational dynamics below the phonon frequency range which can be divided into several dispersion regions. The authors attributed this complicated dispersion to the interaction of polar regions with the soft mode and to the presence of oxygen vacancies. Recent dielectric studies of SrTiO<sub>3</sub> doped with 25% of Bi [12] also revealed a broad dielectric dispersion below room temperature. In contrast to the earlier observations

of the compounds with smaller  $x$  [8, 9], it could be attributed to the dipolar glass systems, i. e. the occurrence of correlated polarization regions with the dimensions greater than several nanometres is not very plausible.

The above-mentioned bulk properties of Sr-based compounds are highly affected by the modifications of their grain boundaries. It was shown by Petzelt et al. [13, 14] that the polar modes, forbidden in bulk SrTiO<sub>3</sub>, develop at the grain boundaries and lead to a grain boundary polarization. This phenomenon was explained as the distortion of tetragonality and the oxygen deficiency in a very thin interface layer. The idea was later supported by the spatially resolved valence-electron energy-loss spectroscopy [15], TEM measurements, and theoretical calculations [16, 17].

Another cause of polarization in Sr-based compounds might be the flexoelectric effect (strain gradient induced polarization [18]). This effect is weak for the most of conventional ferroelectric materials, but for high permittivity materials such as RF [19] or specially prepared composites [20] it can be sufficiently strong. It is known that polar modes can be different at the surfaces of single crystals or grain boundaries of polycrystalline materials from those in the bulk. This can lead to a different behaviour at these interfaces and induce strain gradients which are the main cause of flexoelectric effect. The flexoelectricity studies in SrTiO<sub>3</sub> single crystals [21] and artificially strained layered structures [22] have been investigated by various methods. It was found [21] that the induced polarization can be decomposed into components, directed along different crystallographic directions, and in the vicinity of defects can be comparable with the ferroelectric polarization. Also, the in-plane strain was shown [22] to be the main cause of the out-of-plane flexoelectricity. Since these effects manifest themselves mainly at the surface layer, local piezoelectricity studies of the surface become very important. It has been already shown by piezoresponse force microscopy (PFM) [23] that in undoped SrTiO<sub>3</sub> ceramics the observed piezoelectric contrast can be attributed to the flexoelectric effect caused by the surface relaxation. The observed enhanced piezoresponse at grain boundaries was explained by the inhomogeneous distribution of oxygen vacancies.

These results stimulated us to perform the PFM investigations of Bi-doped SrTiO<sub>3</sub> compounds. First of all, the nature of dielectric relaxation observed in these compounds [12] had to be clarified: either it is dipolar glass-like or similar to that observed in RF. Local piezoelectricity studies would be very helpful here, since the local piezoelectric properties of RF

are quite well explored by PFM (see e. g. [24] and references therein) and it is possible to make a direct comparison of these responses. Also, we assumed that the substitution of Sr by heterovalent atoms such as Bi produces additional vacancy states which will also influence surface strains and, possibly, the flexoelectric response. The comparison between pure and Bi-doped SrTiO<sub>3</sub> could provide us with better understanding of these relations.

## 2. Experiment

The PFM measurements of 0.75SrTiO<sub>3</sub>-0.25BiTiO<sub>3</sub> (SrTiO<sub>3</sub>-Bi) ceramics have been performed using commercial atomic force microscope (*Bruker*, Multimode with Nanoscope IIIA controller) equipped with an external lock-in amplifier (*Stanford Research*, SR-830) and function generator (*Yokogawa*, FG-120). All the measurements were performed on the mirror-polished ceramics. The conducting AFM tip (*Nanosensors*, PPP-NCHR) was brought into a contact with the surface and the local piezoresponse signal was detected as the first harmonic of the tip deflection when the AC field of 5–40 V amplitude and 50 kHz frequency (combined with DC bias voltage 10–40 V) was applied from the function generator. The local piezoresponse loops have been obtained by applying a sequence of pulses and measuring the PFM signal during the time intervals between these pulses. All the data have been collected by using the home-built data acquisition system and LABVIEW analysis software. The obtained PFM images were analysed using the WSxM software [25].

## 3. Results and discussion

The representative topography image and the components of out-of-plane (OPP) and in-plane (IP) PFM signal, acquired by simultaneously applying sinusoidal (AC) and bias (DC) voltage and measuring surface displacements, are presented in Fig. 1. The topography image (Fig. 1(a)) shows a fairly well polished smooth surface (estimated RMS roughness is smaller than 2 nm) with clear polishing scratches which do not correlate with the obtained piezoresponse images (Fig. 1(b, c)). Thus, the influence of surface morphology to the PFM contrast can be ruled out. The scans of out-of-plane as well as in-plane polarization PFM components revealed fairly well polarized areas with the dimensions of a few micrometres. These areas appear nearly at the same positions in OPP and IP images, thus they most likely represent spontaneously polarized grains of the SrTiO<sub>3</sub>-Bi ceramics.

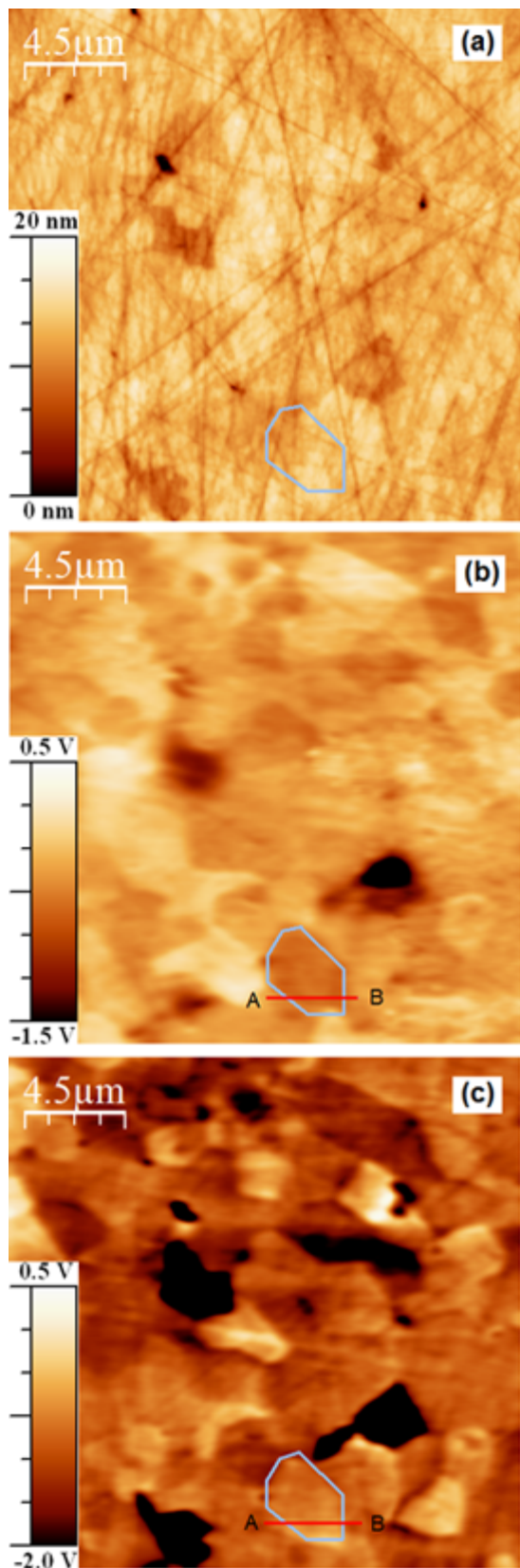


Fig. 1. Surface topography (a), OPP (b), and IP (c) piezoresponse images of  $0.75\text{SrTiO}_3\text{-}0.25\text{BiTiO}_3$  ceramics ( $U_{AC} = 40\text{ V}$ ,  $U_{DC} = 20\text{ V}$ ,  $f = 50\text{ kHz}$ ). The (blue online) contour marks one of the grain boundaries in both OPP and IP images.

The application of a positive bias voltage to the bottom electrode was found to be essential to reveal the apparent PFM signal in this material. This effect is clearly a consequence of Bi-doping because in a pure  $\text{SrTiO}_3$  [23] such bias voltage was not indeed required to obtain clear PFM contrast under the identical conditions. To analyse the piezoelectric signal within individual grains more carefully we plotted the piezoresponse cross-sections across a representative grain along the A-B line in Fig. 1 for both OPP and IP images. One can see that both signals are significantly amplified near the grain boundaries (Fig. 2), this enhancement being especially strong for the IP image.

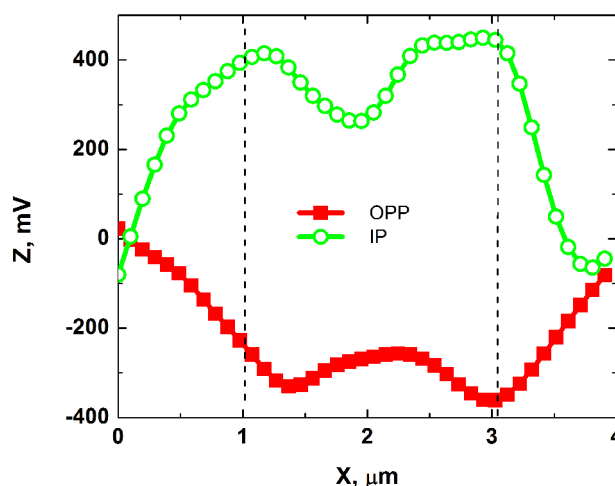


Fig. 2. Cross-section of OPP and IP images along (red online) A-B line in Fig. 1. Dashed lines indicate the grain boundaries.

This result is fully consistent with the analogous observations made for pure  $\text{SrTiO}_3$  [23]. It demonstrates the importance of the grain boundaries to the appearance of piezoresponse in incipient ferroelectrics. The obtained behaviour of piezoresponse substantially deviates from that typically seen in RF where an irregular structure of interpenetrating submicron-sized polarized areas can be clearly indicated within each grain as it was shown in PLZT 9.75/65/35 ceramics [26]. Here we were unable to distinguish any pattern and the distribution of a local polarization is much more uniform. Such a character of piezoresponse indicates that this ceramics might be attributed to the dipolar glass type. In such systems the disorder is known to exist at much smaller scale (up to several lattice units) than the thickness of commercially available AFM cantilevers.

To shed light on the mechanism of the surface piezoelectricity, we plotted PFM contrast distributions within the scanned areas in the form of histograms

(circles in Fig. 3, green online). We found that they are well centred around zero and show slightly asymmetrical shape for both OPP and IP components. This may be related to the existence of several components of the flexoelectric tensor as it was explained in Ref. [23]. The difference with pure SrTiO<sub>3</sub> (squares in Fig. 3, red online) is demonstrated in a narrower distribution that can be a result of the application of bias voltage during the measurement promoting the preferable orientation of some easily polarizable areas in the direction of the applied external field. Another reason could be due to the effect of internal field caused by the oxygen vacancies as will be discussed below. Most probably here we see a superposition of these two factors because neither can be definitely ruled out. Comparing the overall picture with the analogous piezoresponse of pure SrTiO<sub>3</sub> [23] the following common features could be encountered: both OPP and IP components of piezoresponse are present in these materials, the distribution of IP response is broader than that of OPP, and the piezoresponse in single grains increases toward the grain boundaries. The acquired local hysteresis loops appeared to be

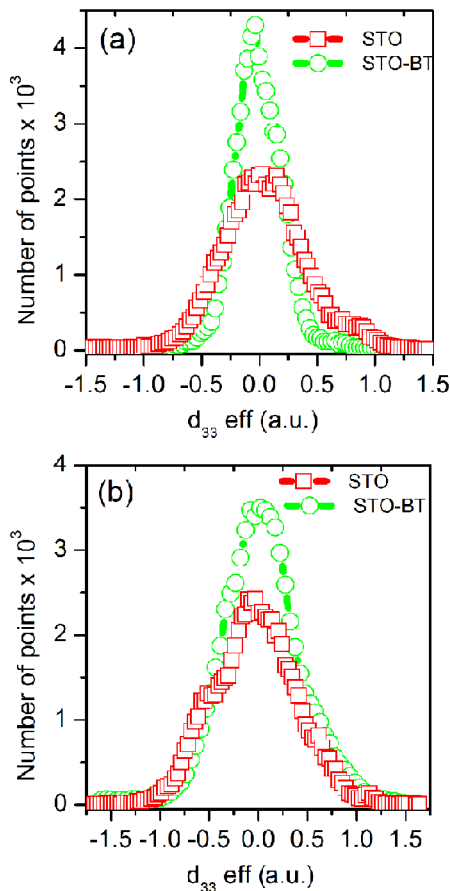


Fig. 3. Histograms of (a) OPP and (b) IP piezoresponse images.

very narrow under sufficiently high electric fields thus confirming the inability to induce any substantial ferroelectric properties even in the middle of the grains. This fact also means that the material possess the properties of dipolar glass (RF can be transformed to ferroelectric state under the applied external electric field). To examine the effect of applied voltage on PFM contrast, we performed a set of scans under varying AC and DC components of applied voltage separately.

The obtained piezoresponse images at several  $U_{AC}$  and  $U_{DC}$  voltages are presented in Fig. 4.

It is easy to see that the decrease of either DC or AC components of applied voltage results in a rapid decrease of PFM contrast. It should be noted that, in contrast to pure SrTiO<sub>3</sub>, the PFM signal can be visible only under positive bias voltage (applied to the bottom electrode). No PFM response can be obtained under negative DC voltage. The quantitative analysis of obtained results was performed by comparing the cross-sections of PFM response of two neighbouring grains exhibiting opposite contrast (along lines in Fig. 4, blue online). The variation of the applied field makes a considerable influence on the PFM signal. This is especially clearly seen in Fig. 5 for the “positive” grain. The detailed analysis of the highest and lowest values of PFM contrast is presented in Fig. 6. Due to the inability to convert measured voltage to piezoelectric coefficient values the piezoresponse was presented in arbitrary units. The piezoelectric nature of PFM response is confirmed by the fact that it is almost a linear function of applied voltage. The response is more susceptible to the AC component of the voltage, and approximately  $U_{AC} = 5$  V is probably the limiting value below which no PFM response is visible. Increasing piezoresponse signals with increasing AC and DC voltage are shown on Fig. 6.

As one of the most probable explanations for the necessity to apply a bias voltage to reveal the piezoresponse signal, the effect of oxygen vacancies should be mentioned. It is known that during substitution of Sr<sup>2+</sup> by Bi<sup>3+</sup> the additional oxygen vacancy states are created to preserve the charge neutrality. Even in pure SrTiO<sub>3</sub> with artificially created oxygen vacancies the change of the resistivity was observed leading to the metallic behaviour [27]. It was suggested that here the structural inhomogeneities and extended defects, which are unavoidable at the surface, play a main role pushing the Fermi level to the conduction band as it was shown by *ab-initio* calculations [28]. In donor-doped systems the regions where oxygen vacancies accumulate become (highly) n-conducting and electrically inhomogeneous. This effect was found especially important in thin films near the surface-electrode layer [29]. As a consequence of this effect, the

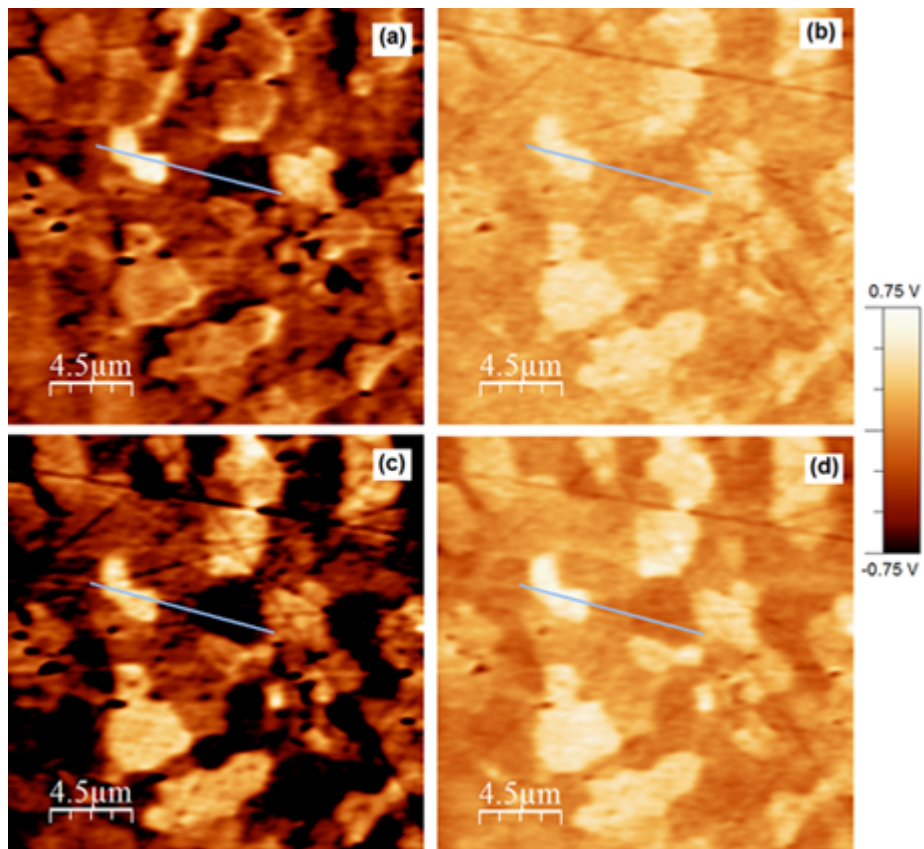


Fig. 4. OPP local piezoresponse data of  $0.75\text{SrTiO}_3\text{-}0.25\text{BiTiO}_3$  ceramic under varying  $U_{AC}$  and  $U_{DC}$ :  $U_{AC} = 40\text{ V}$  (a),  $U_{AC} = 10\text{ V}$  (b) at  $U_{DC} = 20\text{ V}$  and  $U_{DC} = 40\text{ V}$  (c),  $U_{DC} = 10\text{ V}$  (d) at  $U_{AC} = 25\text{ V}$ .

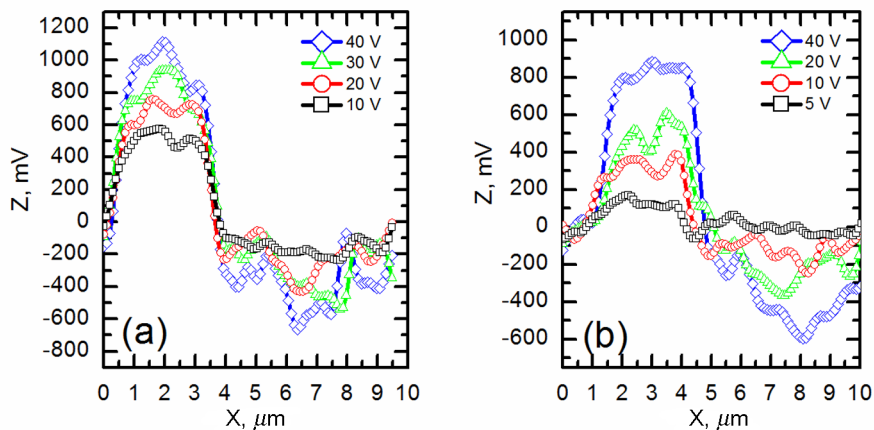


Fig. 5. The cross-sections of piezoresponse images at various (a)  $U_{DC}$  ( $U_{AC} = 25\text{ V}$ ) and (b)  $U_{AC}$  ( $U_{DC} = 20\text{ V}$ ) voltages along (blue online) lines in Fig. 4.

applied electric field significantly decreases at the surface and results in hindering of piezoelectric response by electrical conductivity. The application of a negative DC potential to the cantilever should result in

pushing of negative charge away from the surface and formation of a depleted region. This allows to register the piezoresponse signal by simultaneous application of AC voltage to the tip.

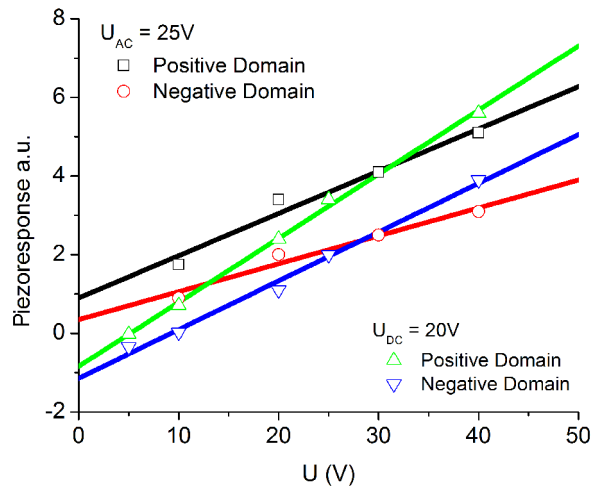


Fig. 6. The analysis of the effective maximum and minimum values of piezoresponse from Fig. 5 under different AC and DC fields.

#### 4. Conclusions

The results demonstrate different nature of the PFM response in  $0.75\text{SrTiO}_3\text{-}0.25\text{BiTiO}_3$  ceramics to compare with that in typical RF like PLZT [26]: no irregular polarized structures can be observed and the piezoresponse contrast is approximately uniform within the grains increasing only at the grain boundaries. Such PFM contrast could be attributed to flexoelectric effect as it was already reported for the pure  $\text{SrTiO}_3$  crystals [23]. Substitution of bivalent Sr by trivalent Bi atoms produces uncompensated charges at the surface of the sample which can be eliminated by application of external bias voltage. This result is very different from that obtained for pure  $\text{SrTiO}_3$ , where a DC bias was not needed to observe the PFM response [23]. Piezoelectric nature of the obtained results is corroborated by existence of both OPP and IP components of the PFM signal and nearly linear dependence of piezoresponse with applied voltage.

#### Acknowledgements

This work was supported by European Union Structural Funds project “Postdoctoral Fellowship Implementation in Lithuania”.

#### References

[1] R. Viana, P. Lunkenheimer, J. Hemberger, R. Bohmer, and A. Loidl, Dielectric spectroscopy in  $\text{SrTiO}_3$ , *Phys. Rev. B* **50**, 601–604 (1994).

[2] G. Shirane and Y. Yamada, Lattice-dynamical study of the  $110^\circ\text{K}$  phase transition in  $\text{SrTiO}_3$ , *Phys. Rev.* **177**, 858–863 (1969).

[3] J.H. Haeni, P. Irvin, W. Chang, R. Uecker, P. Reiche, Y.L. Li, S. Choudhury, W. Tian, M.E. Hawley, B. Craigo, A.K. Tagantsev, X.Q. Pan, S.K. Streiffer, L.Q. Chen, S.W. Kirchoefer, J. Levy, and D.G. Schlom, Room-temperature ferroelectricity in strained  $\text{SrTiO}_3$ , *Nature* **430**, 758–761 (2004).

[4] V.V. Lemanov, E.P. Smirnova, P.P. Syrnikov, and E.A. Tarakanov, Phase transitions and glasslike behavior in  $\text{Sr}_{1-x}\text{Ba}_x\text{TiO}_3$ , *Phys. Rev. B* **54**, 3151–3157 (1996).

[5] J.G. Bednorz and K.A. Müller,  $\text{Sr}_{1-x}\text{Ca}_x\text{TiO}_3$ : an XY quantum ferroelectric with transition to randomness, *Phys. Rev. Lett.* **52**, 2289–2292 (1984).

[6] A. Tkach, P.M. Vilarinho, and A.L. Kholkin, Polar behavior in Mn-doped  $\text{SrTiO}_3$  ceramics, *Appl. Phys. Lett.* **82**, 172902 (2005).

[7] A. Tkach, A. Almeida, J. Agostinho Moreira, T.M. Correia, M.R. Chaves, O. Okhay, P.M. Vilarinho, I. Gregora, and J. Petzelt, Enhancement of tetragonality and role of strontium vacancies in heterovalent doped  $\text{SrTiO}_3$ , *Appl. Phys. Lett.* **98**, 052903 (2011).

[8] G.I. Scanavi, I.J. Ksendzov, V.A. Trigubenko, and V.G. Prokhvatilov, Relaxation polarization and losses in nonferroelectric dielectrics possessing very high dielectric constants, *Zh. Eksp. Teor. Fiz.* **33**, 320 (1957).

[9] V. Porokhonsky, A. Pashkin, V. Bovtun, J. Petzelt, M. Savinov, P. Samoukhina, T. Ostapchuk, J. Pokorný, M. Avdeev, A. Kholkin, and P. Vilarinho, Broad-band dielectric spectroscopy of  $\text{SrTiO}_3$ : Bi ceramics, *Phys. Rev. B* **69**, 144104 (2004).

[10] A. Tkach, P.M. Vilarinho, A.L. Kholkin, I.M. Reaney, J. Pokorný, and J. Petzelt, Mechanisms of the effect of dopants and  $\text{P}(\text{O}_2)$  on the improper ferroelastic phase transition in  $\text{SrTiO}_3$ , *Chem. Mater.* **19**, 6471–6477 (2007).

[11] A. Tkach, T.M. Correia, A. Almeida, J. Agostinho Moreira, M.R. Chaves, O. Okhay, P.M. Vilarinho, I. Gregora, and J. Petzelt, Role of trivalent Sr substituents and Sr vacancies in tetragonal and polar states of  $\text{SrTiO}_3$ , *Acta Mater.* **59**, 5388–5397 (2011).

[12] R. Grigalaitis, J. Banys, S. Bagdzevičius, A. Sternberg, and K. Bormanis, Dielectric investigation of lead-free perovskite strontium titanate with 25% bismuth ceramics, *Phys. Status Solidi C* **6**(12), 2743–2745 (2009).

[13] J. Petzelt, T. Ostapchuk, I. Gregora, I. Rychetsky, S. Hoffmann-Eifert, A.V. Pronin, Y. Yuzyuk, B.P. Gorschunov, S. Kamba, V. Bovtun, J. Pokorný, M. Savinov, V. Porokhonsky, D. Rafaja, P. Vanek, A. Almeida, M.R. Chaves, A.A. Volkov, M. Dressel, and R. Waser, Dielectric, infrared, and Raman response of undoped  $\text{SrTiO}_3$  ceramics: Evidence of polar grain boundaries, *Phys. Rev. B* **64**, 184111 (2001).

- [14] J. Petzelt, T. Ostapchuk, I. Gregora, P. Kuzel, J. Liu, and Z. Chen, Infrared and Raman studies of the dead grain-boundary layers in SrTiO<sub>3</sub> fine-grain ceramics, *J. Phys. Condens. Matter* **19**, 196222 (2007).
- [15] K. van Benthem, G. Tan, L.K. DeNoyer, R.H. French, and M. Ruhle, Local optical properties, electron densities, and London dispersion energies of atomically structured grain boundaries, *Phys. Rev. Lett.* **93**, 227201 (2004).
- [16] R. Shao, M.F. Chisholm, G. Duscher, and D.A. Bonnell, Low-temperature resistance anomaly at SrTiO<sub>3</sub> grain boundaries: evidence for an interface-induced phase transition, *Phys. Rev. Lett.* **95**, 197601 (2005).
- [17] M. Kim, G. Duscher, N.D. Browning, K. Sohlberg, S.T. Pantelides, and S.J. Pennycook, Nonstoichiometry and the electrical activity of grain boundaries in SrTiO<sub>3</sub>, *Phys. Rev. Lett.* **86**, 4056–4059 (2001).
- [18] L.E. Cross, Flexoelectric effects: Charge separation in insulating solids subjected to elastic strain gradients, *J. Mater. Sci.* **41**, 53–63 (2006).
- [19] W. Ma and L.E. Cross, Large flexoelectric polarization in ceramic lead magnesium niobate, *Appl. Phys. Lett.* **79**, 4420–4422 (2001).
- [20] W. Zhu, J.Y. Fu, N. Li, and L.E. Cross, Piezoelectric composite based on the enhanced flexoelectric effects, *Appl. Phys. Lett.* **89**, 192904 (2006).
- [21] P. Zubko, G. Catalan, A. Buckley, P.R.L. Welche, and J.F. Scott, Strain-gradient-induced polarization in SrTiO<sub>3</sub> single crystals, *Phys. Rev. Lett.* **99**, 167601 (2007).
- [22] V. Shelukhin, D. Ehre, E. Lavert, E. Wachtel, Y. Feldman, A. Tagantsev, and I. Lubomirsky, Structural determinants of the sign of the pyroelectric effect in quasi-amorphous SrTiO<sub>3</sub> films, *Adv. Funct. Mater.* **21**, 1403–1410 (2011).
- [23] A. Kholkin, I. Bdikin, T. Ostapchuk, and J. Petzelt, Room temperature surface piezoelectricity in SrTiO<sub>3</sub> ceramics via piezoresponse force microscopy, *Appl. Phys. Lett.* **93**, 222905 (2008).
- [24] A. Kholkin, A. Morozovska, D. Kiselev, I. Bdikin, B. Rodriguez, P. Wu, A. Bokov, Z.-G. Ye, B. Dkhil, L.-Q. Chen, M. Kosec, and S.V. Kalinin, Surface domain structures and mesoscopic phase transition in relaxor ferroelectrics, *Adv. Funct. Mater.* **21**, 1977–1987 (2011).
- [25] I. Horcas, R. Fernández, J.M. Gómez-Rodríguez, J. Colchero, J. Gómez-Herrero, and A.M. Baro, WSXM: A software for scanning probe microscopy and a tool for nanotechnology, *Rev. Sci. Instrum.* **78**, 013705 (2007).
- [26] D.A. Kiselev, I.K. Bdikin, E.K. Selezneva, K. Bormanis, A. Sternberg, and A.L. Kholkin, Grain size effect and local disorder in polycrystalline relaxors via scanning probe microscopy, *J. Phys. Appl. Phys.* **40**, 7109–7112 (2007).
- [27] K. Szot, W. Speier, R. Carius, U. Zastrow, and W. Beyer, Localized metallic conductivity and self-healing during thermal reduction of SrTiO<sub>3</sub>, *Phys. Rev. Lett.* **88**, 075508 (2002).
- [28] N. Shanthi and D.D. Sarma, Electronic structure of electron doped SrTiO<sub>3</sub>: SrTiO<sub>3-δ</sub> and Sr<sub>1-x</sub>La<sub>x</sub>TiO<sub>3</sub>, *Phys. Rev. B* **57**, 2153–2158 (1998).
- [29] M. Dawber, J.F. Scott, and A.J. Hartmann, Effect of donor and acceptor dopants on Schottky barrier heights and vacancy concentrations in barium strontium titanate, *J. Eur. Ceram. Soc.* **21**, 1633–1636 (2001).

## LOKALIOS PJEZOELEKTRINĖS SrTiO<sub>3</sub>-BiTiO<sub>3</sub> KERAMIKŲ SAVYBĖS

R. Grigalaitis<sup>a</sup>, Š. Bagdzevičius<sup>a</sup>, J. Banys<sup>a</sup>, E.E. Tornau<sup>b</sup>, K. Bormanis<sup>c</sup>, A. Sternberg<sup>c</sup>, I. Bdikin<sup>d,e</sup>,  
A. Kholkin<sup>d</sup>

<sup>a</sup> Vilniaus universiteto Fizikos fakultetas, Vilnius, Lietuva

<sup>b</sup> Fizinių ir technologijos mokslų centras, Vilnius, Lietuva

<sup>c</sup> Latvijos universiteto Kietojo kūno fizikos institutas, Ryga, Latvija

<sup>d</sup> Aveiro universiteto Keramikos ir stiklo inžinerijos fakultetas / CICECO, Aveiro, Portugalija

<sup>e</sup> Aveiro universiteto Mechaninės inžinerijos fakultetas / TEMA, Aveiro, Portugalija

### Santrauka

Lokaliuos pjezoelektrinės bismutu praturtintų SrTiO<sub>3</sub> keramikų savybės buvo tyrinėjamos pjezoelektrinės jėgos mikroskopijos metodu. Pjezoelektrinę gautų duomenų prigimtį patvirtino tai, kad buvo stebimos tiek statmenosios, tiek ir lygiagrečiosios bandinio plokštumai poliarizacijos komponentės. Kadangi matuotasis pjezoelektrinis atsakas neparodė jokių „la-

birinto“ tipo struktūrų, prognozuotos feroelektrinio relaksoriaus būsenos šioje medžiagoje aptikti nepavyko. Ženklus lokalių pjezoelektrinių bismutu praturtintų SrTiO<sub>3</sub> keramikų savybių panašumas į grynos SrTiO<sub>3</sub> savybes leidžia daryti prielaidą, kad gautasis pjezoelektrinis atsakas gali būti priskirtas fleksoelektriniam efektui. Praturtinimas bismutu sukelia deguonies vakansijų bei neigiamo krūvio atsiradimą bandinio paviršiuje.